

Supporting Information for

Efficient exploration of compositional space for high-performance copolymers *via* Bayesian optimization

Xinyao Xu[†], Wenlin Zhao[†], Liquan Wang*, Jiaping Lin*, and Lei Du

Shanghai Key Laboratory of Advanced Polymeric Materials, Key Laboratory for Ultrafine Materials of Ministry of Education, Frontiers Science Center for Materiobiology and Dynamic Chemistry, School of Materials Science and Engineering, East China University of Science and Technology, Shanghai, 200237, China

[†]X. X. and W. Z. contributed equally to this work.

*Correspondence and requests for materials should be addressed to J. L. or L.W.

Contents

S1. Simulation method for curing and properties of co-cured polycyanurates	SI 3
S2. Calculated copolymer property space	SI 6
S3. Supplementary results of benchmarking studies and experiments.....	SI 19
References.....	SI 21

S1. Simulation method for curing and properties of co-cured polycyanurates

In this work, the calculated compositional property space of the investigated three-component co-cured cyanate ester (CE) resin was obtained through all-atomic molecular simulations. Unless explicitly stated, the simulation was performed in the simulation box with periodic boundary conditions based on COMPASS force fields, a Nose thermostat, and an Andersen barostat. The default pressure and temperature are 101.325 kPa and 473.15 K, respectively. The particle-particle particle-mesh (PPPM) summation method was used to sum the long-range electrostatic interaction terms, and the direct atom-based method was chosen for the short-range van der Waals interactions. The time step is 1 fs. The steps are as follows.

Step 1. Simulating the curing of CE systems using molecular dynamics (MD) simulations.

We designed a crosslinking scheme based on the cut-off distance criterion and a multi-step relaxation to mimic the cured CE resins¹⁻³, as shown in **Figure S1**. Firstly, three different numbers of CE monomers were placed in a simulation box using an Amorphous Cell module. The total number of cyanate groups in the simulation box is 300, and the mole ratio of each component is constrained by a grid of 1/30. Next, the system was subjected to geometry optimization, and the MD simulation was successively performed under *NPT*, *NVT*, and *NPT* ensembles with 100 ps, 100 ps, and 200 ps, respectively.

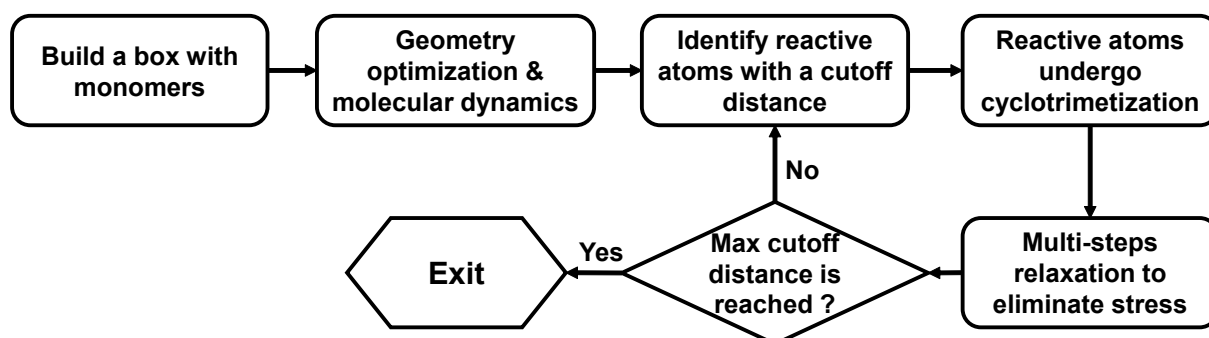


Figure S1. Crosslinking flowchart for co-curing of CE monomers in the MD simulations.

Afterward, the equilibrium configuration was used for the following crosslinking scheme. Only cyclotrimerization of the cyanate group was considered in this procedure. Pairs of reactive atoms (carbon in one cyanate group and nitrogen in another cyanate group) that meet the cut-off distance criterion can be connected by forming new bonds. Bonds and neighboring atoms for the reacted atoms were adjusted, and the total system was subjected to *NPT-NVT-NPT* dynamic simulations with 100-100-100 ps to eliminate internal stress stemming from the cross-linking. The above simulations were repeated until no new pair of reactive atoms were generated within the maximum cut-off distance. To achieve the ultimate degree of crosslinking, we increased the cut-off distance from 3Å to 13Å, where the step is 0.1Å. Under a cut-off distance, only one cyclotrimerization occurs per cycle. When there is no cyclotrimerization occurs, the next cut-off distance is entered.

Step 2. Calculating the hygroscopicity, T_g , and Young's modulus of the cured matrix.

Based on the cross-linked structure of the co-cured CE system obtained by the method in Step 1, we calculated the properties of hygroscopicity, T_g , and Young's modulus of the copolymers.

1) *Hygroscopicity*. Metropolis Monte Carlo (MC) method was used to simulate water molecules absorbed in the cured matrix. The calculation process was realized through the fixed pressure method in the Sorption module⁴. The configurations are sampled from a grand canonical ensemble, and the probability of a configuration, m , is given by

$$\rho_m = CF \left(\{B\}_m \right) \exp[-E_m/k_B T] \quad (\text{S-1})$$

where C is an arbitrary normalization constant, E_m is the total energy of configuration m , k_B is the Boltzmann constant, and T is the temperature.

The adsorption system simulated a 60% relative humidity atmospheric environment at 25 °C. The cross-linked structure of the cocured CE system obtained by the method in Step 1 was subjected to a grand canonical Monte Carlo simulation to place H₂O molecules in energetically favorable locations. The Ewald summation method was used to sum the long-range electrostatic interaction terms. The number of equilibration steps was 20,000,000. And the number of production steps was set to 40,000,000. All unoccupied volumes in the simulation box were considered. The hygroscopicity was

determined by calculating the ratio of the total mass of H₂O molecules absorbed in the sample to the mass of the sample. This calculation was performed using Equation (S-2).

$$\text{hygroscopicity} = \frac{m_{\text{water}}}{m_{\text{sample}}} \times 100\% \quad (\text{S-2})$$

Here, m_{water} is the total mass of the water molecules absorbed in the sample, and the m_{sample} is the mass of the sample.

2) *Glass transition temperature (T_g)*. We used MD simulations to obtain the T_g of the cured matrix. According to the free volume theory⁵, the slope of the volume-temperature curve of polymers changes as the temperature reaches T_g . As such, the T_g is the temperature at the inflection point of the volume-temperature curve. In this work, we recorded the volume of the CE system in the simulation box at various temperatures. The temperature was increased by 10K from 293K to 673K, with the *NPT* dynamics of 200 ps performed at each temperature.

3) *Young's modulus*. We used the constant strain method in the Forcite module to calculate Young's modulus of CE resin⁴. The constant strain method estimates the elastic constant matrix through a series of finite difference approximations. For details, this method involves removing symmetry from the system, followed by a re-optimization of the structure with varying cell parameters. Once the structure is optimized, some strains are applied to create a strained structure. The strained structure is then optimized while keeping the cell parameters fixed, allowing for internal relaxation. The resulting stress is then calculated from the optimized strained structure and used to build a stiffness matrix through a linear fit between the applied strain and the resulting stress patterns. This stiffness matrix is used to predict the mechanical properties of materials such as Young's modulus.

In our simulations, the Ewald summation method has been used to sum the long-range electrostatic interaction terms. The number of steps for each strain was set to 15, and the value of the maximum strain amplitude was set to 0.003.

S2. Calculated copolymer property space

Using the simulation scheme mentioned in Section S1, the calculated copolymer property space (CCPS) was prepared according to the relationship between the formulas and their calculated properties. The values of data points for copolymers in CCPS are given in **Table S1**.

Table S1. Copolymer composition and calculated properties

Composition (mol%)			Hygroscopicity (%)	T_g (°C)	Young's modulus (GPa)
MBCy (1/30)	DOCy (1/30)	BADCy (1/30)			
0	0	30	1.85	200	3.51
0	1	29	1.45	317	3.81
0	2	28	1.53	270	3.61
0	3	27	1.37	286	3.54
0	4	26	1.35	387	3.65
0	5	25	1.42	200	3.77
0	6	24	1.43	330	3.53
0	7	23	1.38	365	3.49
0	8	22	1.27	309	3.69
0	9	21	1.39	300	3.36
0	10	20	0.97	220	3.45
0	11	19	1.18	348	3.38
0	12	18	1.16	345	3.51
0	13	17	1.43	200	3.46
0	14	16	1.22	320	3.23
0	15	15	0.92	331	3.51
0	16	14	1.57	200	3.46
0	17	13	0.96	210	3.61
0	18	12	1.05	299	3.35
0	19	11	0.94	335	3.16
0	20	10	0.90	210	3.16
0	21	9	1.00	313	3.25
0	22	8	0.92	340	3.10
0	23	7	1.13	300	3.30
0	24	6	0.89	260	3.28
0	25	5	1.12	280	3.26
0	26	4	0.85	320	3.09
0	27	3	0.95	210	3.32

(continued Table S1)

0	28	2	0.89	202	3.27
0	29	1	0.91	220	3.39
0	30	0	0.72	250	3.17
1	0	29	1.76	266	3.73
1	1	28	1.36	280	3.47
1	2	27	1.48	330	3.70
1	3	26	1.48	340	3.38
1	4	25	1.48	200	3.76
1	5	24	1.67	317	3.38
1	6	23	1.12	359	3.25
1	7	22	1.52	320	3.30
1	8	21	1.33	200	3.57
1	9	20	1.35	320	3.30
1	10	19	1.32	350	3.23
1	11	18	1.22	380	3.38
1	12	17	1.26	325	3.64
1	13	16	0.80	352	3.92
1	14	15	1.12	200	3.36
1	15	14	1.03	308	3.75
1	16	13	1.21	290	3.47
1	17	12	1.14	283	3.16
1	18	11	0.91	309	3.28
1	19	10	0.93	204	3.59
1	20	9	0.98	210	2.97
1	21	8	1.03	210	3.53
1	22	7	0.86	350	3.52
1	23	6	1.01	211	3.49
1	24	5	1.04	284	3.26
1	25	4	1.05	283	3.38
1	26	3	1.09	280	3.17
1	27	2	1.05	228	3.37
1	28	1	0.68	349	3.23
1	29	0	0.74	370	3.38
2	0	28	1.61	330	3.67
2	1	27	1.62	308	3.65
2	2	26	1.42	260	3.91
2	3	25	1.50	230	3.78
2	4	24	1.57	190	3.61
2	5	23	1.40	355	3.62

(continued Table S1)

2	6	22	1.13	320	3.44
2	7	21	1.45	360	3.54
2	8	20	1.26	200	3.51
2	9	19	1.42	330	3.67
2	10	18	1.25	264	3.35
2	11	17	1.20	301	3.39
2	12	16	1.19	307	3.39
2	13	15	0.98	210	3.23
2	14	14	1.12	220	3.49
2	15	13	1.12	200	3.48
2	16	12	1.05	310	3.44
2	17	11	1.05	264	3.24
2	18	10	1.08	320	3.36
2	19	9	1.07	344	3.54
2	20	8	1.15	337	3.40
2	21	7	1.00	280	3.22
2	22	6	0.97	310	3.44
2	23	5	0.82	292	3.20
2	24	4	0.79	290	3.85
2	25	3	1.07	374	3.28
2	26	2	0.81	210	3.17
2	27	1	0.87	332	3.34
2	28	0	0.79	228	3.24
3	0	27	1.31	362	3.62
3	1	26	1.27	150	3.80
3	2	25	1.13	200	3.58
3	3	24	1.12	280	3.47
3	4	23	1.45	352	3.36
3	5	22	1.36	329	3.70
3	6	21	1.27	290	3.77
3	7	20	1.11	362	3.64
3	8	19	0.94	223	3.49
3	9	18	1.16	370	3.45
3	10	17	1.27	369	3.41
3	11	16	0.98	354	3.30
3	12	15	1.04	280	3.72
3	13	14	1.03	360	3.64
3	14	13	1.04	337	3.42
3	15	12	1.18	320	3.37

(continued Table S1)

3	16	11	0.87	280	3.57
3	17	10	0.83	324	3.21
3	18	9	1.08	236	3.47
3	19	8	1.15	330	3.32
3	20	7	0.94	290	3.24
3	21	6	0.86	314	3.40
3	22	5	0.94	289	3.45
3	23	4	1.09	340	3.29
3	24	3	1.10	323	3.14
3	25	2	0.91	300	3.31
3	26	1	0.90	160	3.29
3	27	0	0.95	268	3.42
4	0	26	0.95	359	3.91
4	1	25	1.04	336	3.41
4	2	24	1.31	298	3.32
4	3	23	1.32	320	3.42
4	4	22	1.12	220	3.50
4	5	21	1.37	220	3.23
4	6	20	1.13	280	3.85
4	7	19	1.19	310	3.39
4	8	18	1.32	317	3.24
4	9	17	1.25	310	3.64
4	10	16	1.06	353	3.18
4	11	15	1.11	367	3.47
4	12	14	1.1	210	3.63
4	13	13	0.95	256	3.41
4	14	12	0.86	290	3.50
4	15	11	1.21	282	3.68
4	16	10	1.00	323	3.56
4	17	9	1.08	230	3.17
4	18	8	0.97	310	3.21
4	19	7	0.94	180	3.39
4	20	6	1.05	276	3.32
4	21	5	0.93	344	3.34
4	22	4	0.82	210	3.48
4	23	3	0.98	340	3.56
4	24	2	0.91	210	3.54
4	25	1	0.90	350	3.31
4	26	0	0.82	338	3.21

(continued Table S1)

5	0	25	1.32	330	3.55
5	1	24	1.44	310	3.48
5	2	23	1.13	196	3.57
5	3	22	1.26	315	3.43
5	4	21	1.16	370	3.92
5	5	20	1.17	356	3.46
5	6	19	1.40	347	3.47
5	7	18	1.18	210	3.49
5	8	17	1.01	348	3.27
5	9	16	1.11	325	3.42
5	10	15	1.14	350	3.50
5	11	14	1.26	270	3.33
5	12	13	1.04	260	3.53
5	13	12	1.14	368	3.36
5	14	11	1.12	267	3.10
5	15	10	0.92	200	3.22
5	16	9	0.87	366	3.27
5	17	8	0.93	336	3.15
5	18	7	1.16	296	3.47
5	19	6	0.99	290	3.37
5	20	5	0.95	322	3.50
5	21	4	0.91	294	3.37
5	22	3	1.08	283	3.35
5	23	2	0.96	290	3.42
5	24	1	0.64	300	3.35
5	25	0	0.75	321	3.01
6	0	24	1.49	348	3.85
6	1	23	1.41	313	3.85
6	2	22	1.13	318	3.43
6	3	21	1.18	210	3.56
6	4	20	1.20	316	3.54
6	5	19	1.30	250	3.45
6	6	18	1.17	347	3.45
6	7	17	1.36	370	3.42
6	8	16	1.26	360	3.63
6	9	15	0.96	320	3.33
6	10	14	1.30	337	3.37
6	11	13	1.14	319	3.45
6	12	12	1.07	300	3.29

(continued Table S1)

6	13	11	0.98	351	3.43
6	14	10	1.05	316	3.58
6	15	9	1.12	360	3.75
6	16	8	1.15	363	3.39
6	17	7	0.87	330	3.38
6	18	6	1.04	210	3.35
6	19	5	0.99	339	3.32
6	20	4	1.10	366	3.41
6	21	3	1.05	322	3.31
6	22	2	0.98	200	3.09
6	23	1	0.95	319	3.54
6	24	0	0.78	310	3.82
7	0	23	1.38	311	3.44
7	1	22	1.03	308	3.52
7	2	21	1.42	280	3.45
7	3	20	1.46	321	3.63
7	4	19	1.45	297	3.67
7	5	18	1.14	240	3.48
7	6	17	1.16	300	3.96
7	7	16	0.98	270	3.34
7	8	15	1.02	346	3.34
7	9	14	1.24	200	3.66
7	10	13	1.10	349	3.76
7	11	12	0.82	240	3.27
7	12	11	1.14	305	3.53
7	13	10	0.84	277	3.43
7	14	9	0.92	335	3.51
7	15	8	1.03	316	3.43
7	16	7	0.98	316	3.17
7	17	6	0.89	347	3.73
7	18	5	0.82	340	3.23
7	19	4	0.90	200	3.87
7	20	3	0.99	240	3.47
7	21	2	0.97	276	3.45
7	22	1	1.02	381	3.51
7	23	0	0.82	160	3.4
8	0	22	1.50	346	3.99
8	1	21	1.08	270	3.67
8	2	20	1.41	343	3.53

(continued Table S1)

8	3	19	1.20	281	3.61
8	4	18	1.15	315	3.38
8	5	17	1.44	275	3.36
8	6	16	1.00	310	3.39
8	7	15	1.15	310	3.43
8	8	14	1.10	280	3.62
8	9	13	1.07	292	3.29
8	10	12	1.04	340	3.55
8	11	11	1.21	293	3.54
8	12	10	1.00	300	3.11
8	13	9	0.85	348	3.61
8	14	8	0.99	290	3.42
8	15	7	1.07	340	3.61
8	16	6	1.13	314	3.11
8	17	5	1.01	247	3.34
8	18	4	0.77	296	3.33
8	19	3	0.86	320	3.57
8	20	2	0.72	329	3.25
8	21	1	1.07	288	3.39
8	22	0	0.82	290	3.45
9	0	21	1.4	356	3.51
9	1	20	0.95	280	3.67
9	2	19	1.5	90	3.70
9	3	18	1.18	320	3.81
9	4	17	1.03	310	3.28
9	5	16	0.81	280	3.56
9	6	15	0.92	324	3.61
9	7	14	0.96	335	3.45
9	8	13	0.96	163	3.41
9	9	12	1.04	300	3.62
9	10	11	0.89	355	3.61
9	11	10	1.08	339	3.31
9	12	9	1.00	313	3.39
9	13	8	0.90	328	3.72
9	14	7	0.89	260	3.29
9	15	6	0.99	330	3.54
9	16	5	0.83	330	3.24
9	17	4	0.95	270	3.51
9	18	3	0.72	331	3.42

(continued Table S1)

9	19	2	0.93	350	3.32
9	20	1	0.93	364	3.27
9	21	0	0.77	297	3.22
10	0	20	1.23	308	3.53
10	1	19	1.00	315	3.73
10	2	18	1.26	90	3.65
10	3	17	1.11	300	3.39
10	4	16	1.04	290	3.45
10	5	15	1.05	310	3.36
10	6	14	1.10	320	3.24
10	7	13	1.07	210	3.61
10	8	12	1.38	252	3.28
10	9	11	1.03	297	3.72
10	10	10	0.88	330	3.37
10	11	9	0.99	211	3.41
10	12	8	0.93	340	3.36
10	13	7	0.84	320	3.42
10	14	6	1.08	306	3.50
10	15	5	0.98	200	3.06
10	16	4	1.10	386	3.23
10	17	3	0.85	240	3.50
10	18	2	0.93	272	3.48
10	19	1	0.91	331	3.16
10	20	0	0.81	300	3.30
11	0	19	1.11	338	3.51
11	1	18	1.00	309	3.27
11	2	17	0.94	276	3.46
11	3	16	1.02	240	3.40
11	4	15	1.21	287	3.63
11	5	14	1.04	331	3.45
11	6	13	1.00	296	3.38
11	7	12	1.21	370	3.40
11	8	11	1.01	340	3.66
11	9	10	1.05	281	3.36
11	10	9	1.02	360	3.45
11	11	8	0.94	330	3.13
11	12	7	0.97	308	3.37
11	13	6	0.83	275	3.55
11	14	5	1.14	280	3.47

(continued Table S1)

11	15	4	1.08	340	3.39
11	16	3	0.99	290	3.20
11	17	2	0.84	367	3.47
11	18	1	0.82	220	3.14
11	19	0	0.73	310	3.33
12	0	18	0.95	311	3.29
12	1	17	1.04	329	3.57
12	2	16	1.10	310	3.63
12	3	15	1.12	309	3.80
12	4	14	1.22	376	3.63
12	5	13	1.02	305	3.81
12	6	12	0.95	327	3.37
12	7	11	0.86	360	3.18
12	8	10	0.93	310	3.65
12	9	9	1.00	297	3.53
12	10	8	0.98	360	3.21
12	11	7	0.93	331	3.36
12	12	6	1.07	330	3.33
12	13	5	1.11	325	3.46
12	14	4	0.98	207	3.58
12	15	3	0.84	260	3.30
12	16	2	0.85	310	3.34
12	17	1	0.65	310	3.53
12	18	0	0.84	369	3.27
13	0	17	1.21	250	3.69
13	1	16	1.01	299	3.66
13	2	15	1.03	307	3.76
13	3	14	0.97	290	3.75
13	4	13	1.11	322	3.56
13	5	12	0.81	374	3.52
13	6	11	1.10	320	3.62
13	7	10	1.05	150	3.44
13	8	9	1.04	290	3.54
13	9	8	0.98	290	3.53
13	10	7	0.96	312	3.48
13	11	6	0.91	299	3.52
13	12	5	0.83	322	3.33
13	13	4	0.75	339	3.45
13	14	3	0.92	265	3.16

(continued Table S1)

13	15	2	0.95	320	3.53
13	16	1	0.93	320	3.65
13	17	0	0.82	324	3.10
14	0	16	0.97	347	3.39
14	1	15	0.84	277	3.64
14	2	14	0.94	284	3.42
14	3	13	1.07	357	3.63
14	4	12	0.69	320	3.66
14	5	11	0.94	329	3.60
14	6	10	1.08	330	3.50
14	7	9	0.89	367	3.31
14	8	8	0.98	330	3.16
14	9	7	0.86	210	3.50
14	10	6	0.74	290	3.56
14	11	5	0.84	363	3.52
14	12	4	0.85	338	3.46
14	13	3	0.81	340	3.34
14	14	2	0.87	295	3.33
14	15	1	0.73	280	3.50
14	16	0	0.94	320	3.43
15	0	15	1.04	270	3.30
15	1	14	0.91	320	3.57
15	2	13	0.93	320	3.54
15	3	12	0.98	310	3.57
15	4	11	0.87	289	3.47
15	5	10	1.07	309	3.40
15	6	9	1.08	323	3.63
15	7	8	0.85	210	3.17
15	8	7	0.82	286	3.25
15	9	6	0.90	317	3.39
15	10	5	0.77	310	3.52
15	11	4	0.79	334	3.58
15	12	3	0.81	327	3.43
15	13	2	0.96	280	3.28
15	14	1	0.78	346	3.43
15	15	0	0.96	332	3.26
16	0	14	1.21	280	3.54
16	1	13	0.77	310	3.78
16	2	12	1.02	288	3.36

(continued Table S1)

16	3	11	0.78	340	3.47
16	4	10	1.00	318	3.53
16	5	9	0.86	313	3.59
16	6	8	0.77	310	3.85
16	7	7	1.09	300	3.42
16	8	6	0.95	324	3.44
16	9	5	0.61	321	3.23
16	10	4	0.78	325	3.13
16	11	3	0.85	314	3.29
16	12	2	0.78	310	3.25
16	13	1	0.85	304	3.44
16	14	0	0.70	354	3.30
17	0	13	0.95	327	3.62
17	1	12	0.95	310	3.56
17	2	11	0.86	308	3.52
17	3	10	0.80	300	3.50
17	4	9	0.78	335	3.72
17	5	8	1.06	320	3.66
17	6	7	0.86	327	3.44
17	7	6	1.00	310	3.30
17	8	5	1.05	331	3.35
17	9	4	1.03	301	3.37
17	10	3	0.73	372	3.58
17	11	2	0.68	330	3.59
17	12	1	1.04	354	3.40
17	13	0	0.72	280	3.22
18	0	12	1.03	329	3.38
18	1	11	0.96	314	3.21
18	2	10	1.12	309	3.54
18	3	9	0.97	327	3.43
18	4	8	0.78	293	3.23
18	5	7	0.98	336	3.54
18	6	6	0.88	338	3.69
18	7	5	0.86	320	3.45
18	8	4	0.93	274	3.45
18	9	3	0.83	340	3.24
18	10	2	0.81	356	3.16
18	11	1	0.86	311	3.3
18	12	0	0.86	320	3.24

(continued Table S1)

19	0	11	0.84	318	3.34
19	1	10	0.94	324	3.56
19	2	9	0.97	307	3.75
19	3	8	0.83	280	3.69
19	4	7	0.96	313	3.39
19	5	6	0.78	300	3.31
19	6	5	0.49	306	3.35
19	7	4	0.92	320	3.60
19	8	3	0.79	330	3.34
19	9	2	0.64	347	3.10
19	10	1	0.74	309	3.19
19	11	0	0.77	330	3.47
20	0	10	0.86	328	3.72
20	1	9	0.88	304	3.46
20	2	8	0.78	340	3.53
20	3	7	0.94	301	3.38
20	4	6	1.17	300	3.61
20	5	5	0.84	350	3.37
20	6	4	0.80	292	3.34
20	7	3	0.84	338	3.75
20	8	2	0.73	320	3.50
20	9	1	0.90	354	3.44
20	10	0	0.70	320	3.44
21	0	9	0.96	280	3.41
21	1	8	0.76	280	3.53
21	2	7	0.87	329	3.53
21	3	6	0.69	339	3.63
21	4	5	0.65	282	3.72
21	5	4	0.96	270	3.52
21	6	3	0.90	339	3.61
21	7	2	0.82	279	3.70
21	8	1	0.85	316	3.77
21	9	0	0.77	326	3.32
22	0	8	0.80	281	3.57
22	1	7	0.77	325	3.56
22	2	6	0.88	289	3.41
22	3	5	0.86	290	3.59
22	4	4	0.74	281	3.50
22	5	3	0.70	307	3.65

(continued Table S1)

22	6	2	0.74	290	3.56
22	7	1	0.87	309	3.59
22	8	0	0.75	310	3.56
23	0	7	0.95	307	3.49
23	1	6	0.80	310	3.56
23	2	5	0.90	340	3.21
23	3	4	0.84	301	3.36
23	4	3	0.75	321	3.59
23	5	2	0.94	314	3.41
23	6	1	0.79	320	3.39
23	7	0	0.75	333	3.28
24	0	6	0.79	290	3.55
24	1	5	0.84	315	3.47
24	2	4	0.77	337	3.64
24	3	3	0.90	308	3.17
24	4	2	0.82	310	3.38
24	5	1	0.74	355	3.68
24	6	0	0.84	299	3.11
25	0	5	0.75	320	3.56
25	1	4	0.81	286	3.58
25	2	3	0.77	306	3.12
25	3	2	0.79	280	3.71
25	4	1	0.62	320	3.53
25	5	0	0.78	267	3.36
26	0	4	0.87	304	3.46
26	1	3	0.84	280	3.52
26	2	2	0.91	292	3.28
26	3	1	0.78	276	3.31
26	4	0	0.54	310	3.70
27	0	3	0.63	282	3.37
27	1	2	0.69	285	3.40
27	2	1	0.84	296	3.66
27	3	0	0.70	324	3.35
28	0	2	0.56	330	3.77
28	1	1	0.71	326	3.58
28	2	0	0.74	324	3.58
29	0	1	0.75	317	3.49
29	1	0	0.76	328	3.67
30	0	0	0.77	260	3.70

S3. Supplementary results of benchmarking studies and experiments

This section provides supplementary results of benchmarking studies and experimental design during the iterative process. **Figure S2** shows the data points in calculated copolymer property space (CCPS) plotted as a function of hygroscopicity, T_g , and Young's modulus. The sample points in CCPS are colored based on the scores calculated by a) Score_{WS} , b) Score_{WL} , and c) Score_{WP} , respectively.

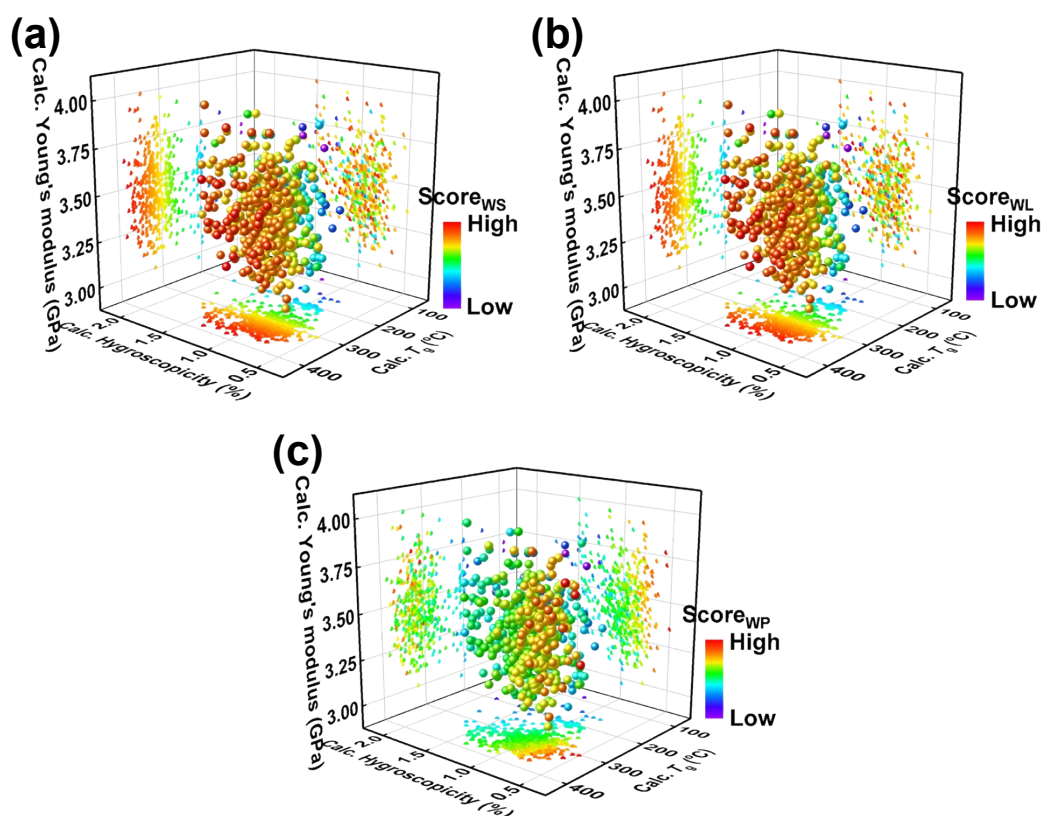


Figure S2. Plots of CCPS. The sample points are colored based on the score calculated by a) Score_{WS} , b) Score_{WL} , and c) Score_{WP} . The point with a high score tends to be red.

Figure S3 shows two plots illustrating the iterative curves of benchmarking studies guided by a combination of $k_{\#1}$ and EI. The plots show the a) best ranking and b) best score in samples as a function of iteration and show data for five example groups among 500 replicates, along with the average of 500 replicates. **Figure S4** shows the standard error of the best ranking during iteration. The contour of a) overall scores and b) EI values of compositional space during the iteration are given in **Figure S5**.

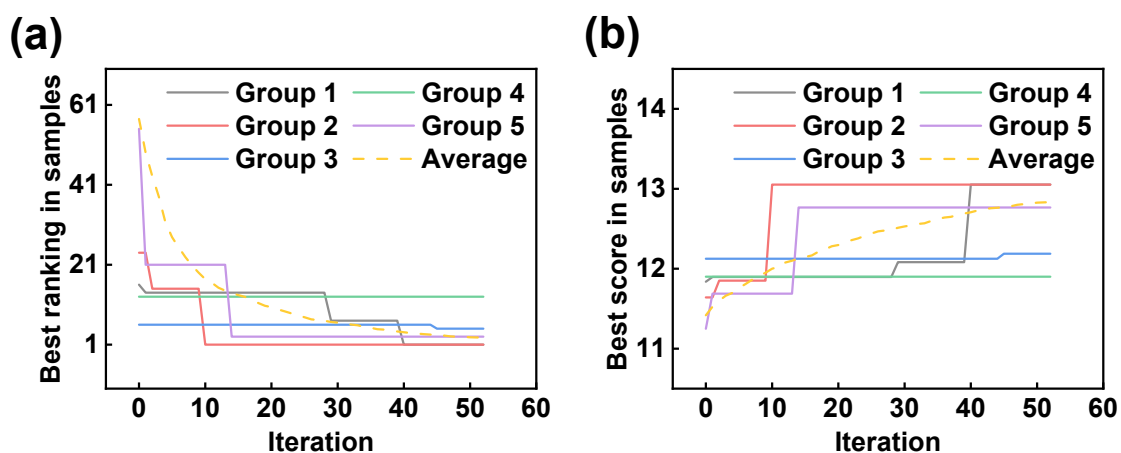


Figure S3. Iterative curves guided by $k_{\#1}$ and EI. The a) best ranking and b) best score for samples are plotted as a function of iteration ($N_{\text{initial}}=12$, $N_{\text{infill}}=1$). Five examples among 500 replicates and the average of 500 replicates are shown.

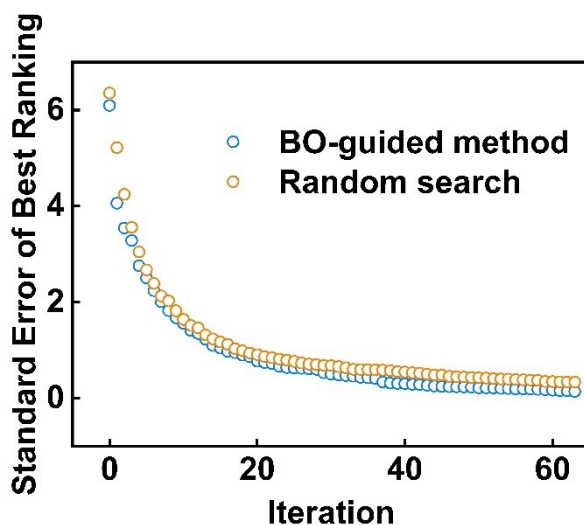


Figure S4. The standard error of the best ranking during iteration.

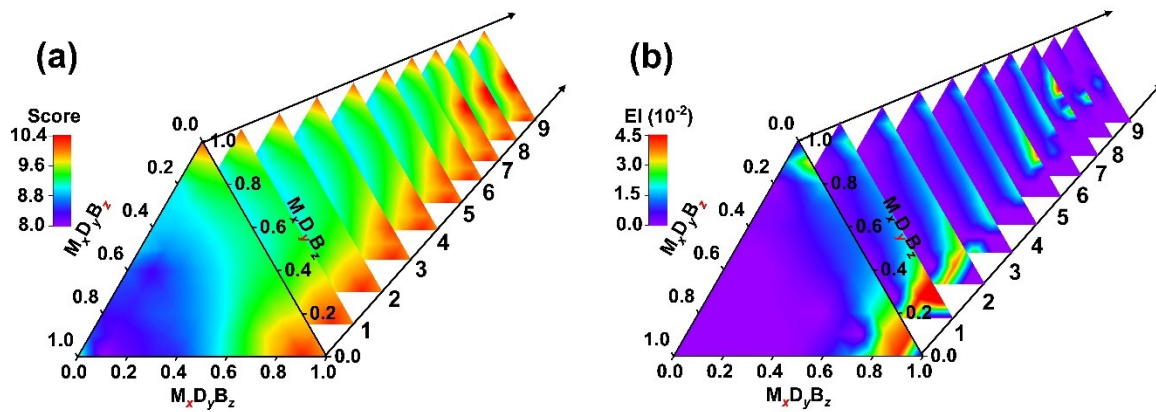


Figure S5. The contour of a) overall scores and b) EI values during the iteration.

References

- (1) Zhu, J.; Chu, M.; Chen, Z.; Wang, L.; Lin, J.; Du, L. Rational Design of Heat-Resistant Polymers with Low Curing Energies by a Materials Genome Approach. *Chem. Mater.* **2020**, *32*, 4527-4535.
- (2) Radue, M. S.; Varshney, V.; Baur, J. W.; Roy, A. K.; Odegard, G. M. Molecular Modeling of Cross-Linked Polymers with Complex Cure Pathways: A Case Study of Bismaleimide Resins. *Macromolecules* **2018**, *51*, 1830-1840.
- (3) Varshney, V.; Patnaik, S. S.; Roy, A. K.; Farmer, B. L. A Molecular Dynamics Study of Epoxy-Based Networks: Cross-Linking Procedure and Prediction of Molecular and Material Properties. *Macromolecules* **2008**, *41*, 6837-6842.
- (4) BIOVIA Materials Studio. <https://www.3ds.com/products-services/biovia/products/molecular-modeling-simulation/biovia-materials-studio/>.
- (5) Ramesh, N.; Davis, P. K.; Zielinski, J. M.; Danner, R. P.; Duda, J. L. Application of Free-Volume Theory to Self Diffusion of Solvents in Polymers Below the Glass Transition Temperature: A Review. *J. Polym. Sci. Pol. Phys.* **2011**, *49*, 1629-1644.